

Performance of the MACE-MP-0 potential for calculating viscosity in LiF molten salt.

H. L. Devereux,¹ M. Withington,¹ C. Cockrell,² K. Trachenko,¹ and A. M. Elena³

¹*School of Physical and Chemical Sciences, Queen Mary University of London, Mile End Road, London, E1 4NS, UK*

²*Nuclear Futures Institute, Bangor University, Bangor, LL57 1UT, UK*

³*Scientific Computing Department, Science and Technology Facilities Council, Daresbury Laboratory, Keckwick Lane, Daresbury, WA4 4AD, UK*

We perform molecular dynamics simulations of molten Lithium Fluoride using the MACE-MP-0 (small machine learnt interatomic potential and the classical Buckingham and Born-Huggins-Mayer potentials. We find that the MACE-MP-0, out-of-the-box, is able to accurately reproduce the experimental viscosity across the liquid state. Whilst the previous predicted viscosities from classical potentials are under-predicted, which has previously been attributed to a suppressed melting temperature. We find that the melting temperature simulated by MACE-MP-0, simply by heating a crystal structure, is significantly closer to the experimental melting temperature of LiF.

1. INTRODUCTION

Molten salts such as LiF have received long term and recent interest due to their use in solar cells, as electrolytes and solvents¹, and potential utilisation as coolant fluids in nuclear reactors, along with metals²⁻⁵. Water is the usual coolant in these nuclear applications but suffers from a high-reactivity⁶. In addition to the use of molten salts as a coolant in the reactor, there are proposals to use the salt as a carrier for the fuel, by dissolving the fuel into the salt. This would allow for adjustments to be made without unloading the core and reduce the amount of nuclear waste generated^{7,8}. Molten salts can host pyroprocessing reactions with very high activity nucleides to increase fuel efficiency and reduce waste generation⁸⁻¹². Furthermore, molten salts have seen use as thermal storage media to complement renewable energy sources, with research interest growing in recent years¹³⁻¹⁶.

A thorough understanding of the thermodynamic and transport properties of molten salts and their mixtures will underlie the upscaling of the above processes to industrial scales, however this understanding is hindered by a poor theoretical understanding of the liquid state¹⁷⁻¹⁹, and the inadequacy of classical atomistic models in generating faithful thermophysical data^{20,21}.

Viscosity is one key property governing the performance of working fluids in thermal hydraulics, which has been investigated theoretically in relation to its temperature dependent minimum that may be related to fundamental physical constants^{17,22}. Previously we investigated this minimum in LiF using classical molecular dynamics (MD)²³ where, as found elsewhere²⁴, the Buckingham potential model of molten LiF²⁴⁻²⁷ predicts the viscosity at a noticeable off-set temperature. Ciccotti *et al.* reported a slightly better agreement using the Born-Huggins-Mayer (BHM) potential and by analysing the response to an explicit shearing force for one temperature point²⁸ as far back as 1976.

Motivated by these applications and a desire to im-

prove the MD picture of molten LiF we now turn to the rapidly growing field of machine-learnt interatomic potentials (MLIPs). The MACE-MP-0 (MACE) MLIP^{29,30} is one example which has seen diverse successes across atomistic material modelling³¹. Here we report the accuracy of viscosity values calculated using the MACE potential against experimental viscosity data.

2. METHODS

We perform MD simulations of molten LiF using classical MD (using the Buckingham and BHM potentials), *via* the DL_POLY package³², and MACE MLIP^{29,30}, *via* the python package janus-core³³ using MACE_MP_0 (small flavour). In both cases we use the Green-Kubo method³⁴⁻³⁶ to calculate viscosity from the integral

$$\eta = \frac{V}{k_B T} \int_0^\infty dt \langle \sigma_{xy}(t) \sigma_{xy}(0) \rangle, \quad (1)$$

where $\langle \cdot \rangle$ is the ensemble average, T is the mean system temperature and k_B is Boltzmann's constant. Equation 1 may be calculated using DL_POLY's on-the-fly correlator. The stress tensor is defined as

$$\sigma_{\alpha\beta} = \frac{1}{V} \sum_i m^i v_\alpha^i v_\beta^i - \frac{1}{V} \sum_{i,j \neq i} r_\alpha^{ij} F_\beta^{ij}, \quad (2)$$

where α and β are Cartesian component indices, m^i , v^i , r^i are particle i 's mass, velocity, and position, and $\mathbf{r}^{ij} = \mathbf{r}^i - \mathbf{r}^j$, \mathbf{F}^{ij} is the force on i due to j and V is the system volume. Finally, x and y are orthogonal Cartesian coordinates. We also compute the average viscosity utilising the other off-diagonal terms, $z-x$ and $y-z$, analogously to Equation 1. We also use the python package ASE³⁷ to calculate the partial radial distribution functions (RDFs), $g(r)$. Then to calculate the structure fac-

tor we use³⁸

$$S(k) = 1 + 4\pi n \int_0^\infty dr r^2 [g(r) - 1] \frac{\sin kr}{kr}, \quad (3)$$

with n the number density.

For accurate viscosity statistics a long simulation runtime is required as well as a sufficient number of independent samples^{23,24,36,39}. For all statistics collection simulations we use the NVE ensemble with a timestep of 1 fs and a trajectory length of 1 ns, and average across 20 initial configurations each independently initialised with the same density. For equilibration we heat the system in the NPT ensemble from a crystal lattice structure taking temperature steps from 10 K to the desired temperature in steps of 50 K. Each subsequent heating step lasts for 10 ps, except when determining the melting point, in proximity to which we simulate for 50 ps. We perform a final 10 ps equilibration at each temperature with 20 different initial velocity seeds in the NVE ensemble before production runs.

The viscosities calculated from Eq. 1 are compared to experimental values of viscosity^{40–43}. For both MD methods we use the same maximum correlation time for calculating η , 5 ps. Janus-core is able to make use of MACE GPU hardware acceleration for calculations, however the added computational complexity of the many-bodied MACE potential stills leads to a far longer simulation wall-time (typically one order of magnitude) than the CPU based DL_POLY calculations based on classical potentials. In both we use a system size of $N = 512$ atoms, where we have previously found little impact on results from utilising large system sizes up to 100000 atoms for classical potentials in LiF²³ and Argon³⁹ systems.

For the Buckingham and BHM potentials we use standard parameters for LiF stemming from the methods of Tosi and Fumi for the alkali halides of NaCl-type^{24,26–28}. Ignoring electrostatics, in DL_POLY the Buckingham and BHM potentials have the form

$$U_{\text{Buckingham}}(r) = Ae^{-\frac{r}{\rho}} - \frac{C}{r^6}, \quad (4)$$

$$U_{\text{BHM}}(r) = Ae^{B(\sigma-r)} - \frac{C}{r^6} - \frac{D}{r^8}, \quad (5)$$

for parameters A, B, σ, ρ, C , and D and inter-atomic distance r . The parameters for all of the interactions are given in table I. When performing our simulations in DL_POLY we also use the Smooth-particle Mesh Ewald method for electrostatic interactions⁴⁴.

The MACE model relies upon a Message Passing Neural-Network (MPNN) architecture where the input space is the dynamic local environment around any given atom along with its static properties (e.g. chemical element). Messages are constructed with radial basis functions and spherical harmonics to encode known symmetries in physical applications. Importantly the MACE model utilises higher-order many-body ACE expansion⁴⁵

Buckingham	Li-Li	Li-F	F-F
A [eV]	98.92	228.99	420.48
ρ [Å]	0.299	0.299	0.299
C [Å ⁶ eV]	0.046	0.499	9.051
BHM			
A [eV]	0.422	0.290	0.158
B [Å ⁻¹]	3.344	3.344	3.344
σ [Å]	1.632	1.995	2.358
C [Å ⁶ eV]	0.0456	0.499	9.050
D [Å ⁸ eV]	0.019	0.374	10.610

TABLE I. Buckingham and BHM potential parameters (in DL_POLY format) corresponding to Equations 4 and 5 to three decimal places.

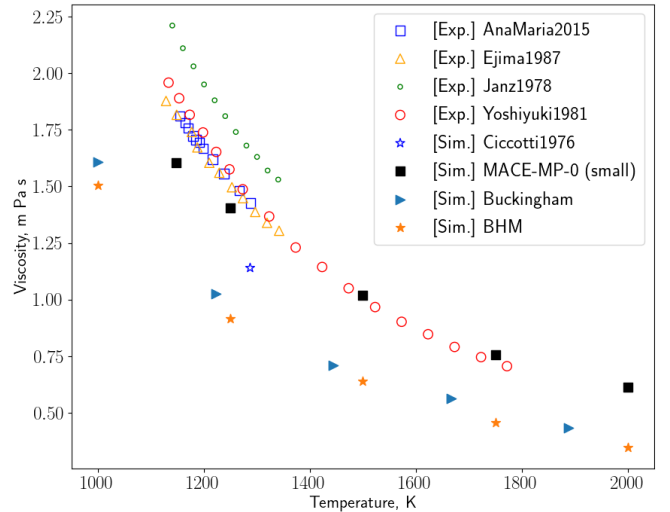


FIG. 1. Viscosity, η , from experimental results^{40–43} and calculated results using the MACE,²⁸ BHM and Buckingham potential. As reported previously for LiF^{23,24}, the Buckingham potential has the correct trend but is off-set on the temperature axis. The MACE results show good agreement with experimental results.

for message passing to achieve faster and more accurate convergence to ground-truth Density Functional Theory (DFT) energies, forces, and stresses than other similar schemes to build MLIPs. The model is trained upon the MPtrj data set introduced for CHGNet⁴⁶ and compiled from the Material Project dataset⁴⁷, which includes 89 elements (including Li and F) in $\sim 146,000$ materials. Not all the MLIPs are suitable for molecular dynamics studies since not all possess conservative forces and stresses. MACE, however, is a conservative model⁴⁸.

3. RESULTS AND DISCUSSION

We begin by comparing the viscosity measurements from the three computational models to experimental

data in Figure 1. The results for the MACE model agree well with the experimental data across the temperature axis, unlike the known offset for the Buckingham and BHM models: the simulated viscosity matches the experimental viscosity well, albeit with the latter at a temperature around 300 K higher.

Previously, the offsetting of viscosity values in the Buckingham results have been ascribed to the model undergoing melting at a suppressed temperature value commensurate with the gap between the simulated and experimental viscosity data²⁴. To investigate this, in Figure 2 we show the system volume V for the MACE, Buckingham, and BHM models following a gradual monotonic heating from a crystal structure up to 1250 K. We observe good agreement between the experimental melting temperature and the melting temperature of the MACE simulation. This supports this notion that the poor reproduction of the experimental viscosity in simulations governed by the Buckingham and BHM models is related to the underestimation of the the melting temperature by approximately 300 K, ascertained in experiments to be 1121 K^{49,50} (although 1143 K is also recorded⁵¹).

It should be noted that there are several factors contributing to the location of melting point in molecular simulations. For example, simulated systems often employ periodic boundary conditions and hence have no free surfaces or interfaces, present experimentally, which promote melting. Another factor is the small system sizes in MD simulations compared to experiments. This leads to the absence of long-wavelength and low-frequency phonons with large displacement amplitudes which destabilise the solid structure and likewise encourage melting. For these and other reasons, gradual heating from a crystal structure might not be generally accurate for determining the melting point⁵²⁻⁵⁴ and other methods such as calculating the free energies of solid and liquid phases, simulating phase co-existence and so on⁵⁵ can be used instead. The performance of MACE potentials for determining the melting point can be tested using these approaches, however the goal and emphasis of this work is the calculation and prediction of transport properties such as viscosity rather than determining the melting point accurately which is a task for future investigations. Furthermore, the very large underestimation of the melting line by the classical potentials means the crude method we employ here is informative in gauging the improvement of the MLIP. It is nevertheless interesting to observe the good agreement between modelling and experimental melting point in Figure 2.

Given the accuracy of the viscosity results of the MACE model we also examine the resulting structure and dynamics, to determine if they are physically reasonable. First we show the velocity autocorrelation functions (VAFs) of the Buckingham and MACE models in figure 3, with the resultant densities of states (DOS) of each included as insets. We calculate these values just above the melting points in each case to compare the dynamics at the lowest temperature still consistent with the liquid

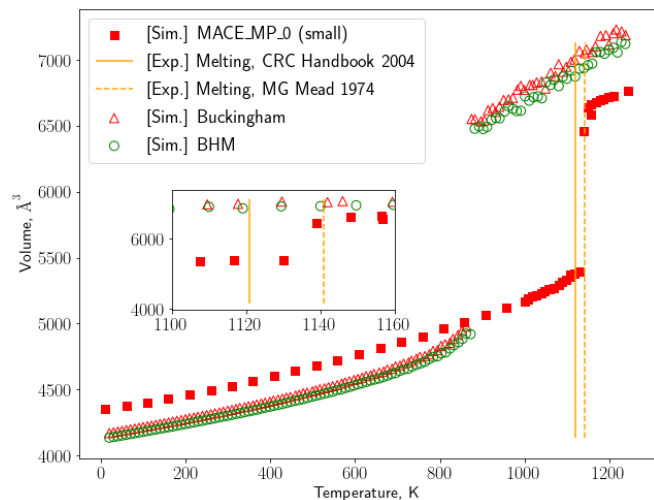


FIG. 2. Volume from heating LiF from a crystal structure from 10 K up to 1250 K, with inset showing the melting point in more detail. The melting point is more accurately determined by the MACE potential than the Buckingham potential. CF the off setting of the viscosity data along the temperature axis in Figure 1. The offset of the melting point in temperature is approximately the same (200-300 K).

state. Our DL_POLY results for LiF are consistent with previous MD results⁵⁶. The results for the MACE potential are significantly different from those of the Buckingham model. We see a decrease of the well known oscillatory frequency of F and particularly Li atoms in the MACE simulation. Both Li and F atoms exhibit a much deeper minima in the MACE VAFs, approximately equal in magnitude. Furthermore the shapes of their respective VAFs are very similar, whereas there are clear qualitative differences in the classical VAFs. The VAF minima and their depth are associated with the solidlike oscillatory component of liquid dynamics, whereas the absence of the minima signals the disappearance of the oscillatory component and purely gaslike dynamics⁵⁷. In this sense, deeper minima in MACE systems imply more pronounced solidlike component of the liquid motion.

Next we look at the partial RDFs $g(r)$ in Figure 4, and the structure factors derived from them in Figure 5. We show $g(r)$ for each pair at the approximate melting temperature of each potential. The first and second peaks of each model are located at approximately the same radial separation, with the MACE peak heights slightly lower and the peak positions slightly higher than those of the classical RDFs. The reduction in magnitude indicates a somewhat broader coordination environment simulated by the MACE model than the classical model, which may be related to the lower frequency oscillation of the Li ions in the MACE simulation. In Figure 4 we can clearly see the first two peaks for each of the partial RDFs. In order to increase the calculation cutoff radius and see the peaks reduce further and the $g(r)$ tend to 1 we would need a larger system. For the computational time and power

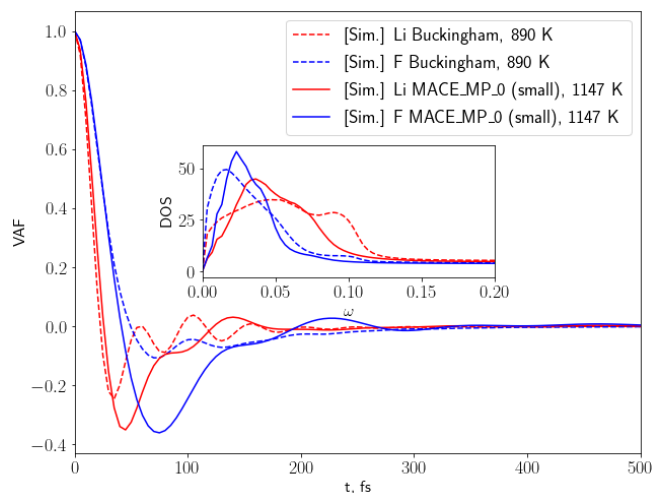


FIG. 3. (a) VAFs for the Buckingham potential and MACE, along with the respective Density of States (DOS). The temperatures of 890 K and 1147 K were chosen to compare the VAFs just above the melting points of the Buckingham and MACE potentials respectively. The DOS were calculated using lag times up to 1,500 fs.

we have available this is not practical with MACE-MP-0. Although limited by the cut-off, the overall shape and location of peaks of $S(k)$ and $g(r)$ is consistent with the expected results for LiF simulated with MD^{56,58}.

An interesting insight from the RDF analysis is that average structures can be quite similar, yet dynamics and transport properties can differ substantially as we saw for viscosity results earlier. This underscores the point which is perhaps not unexpected: similar equilibrium separations may or may not involve similar stiffness of the interatomic potentials which set the local activation energies and transport properties.

4. CONCLUSIONS

We have investigated the performance of the MACE MLIP applied to the MD modelling of the molten salt LiF. The MACE potential is able to more accurately reproduce experimental properties of molten LiF, but at the cost of an increased computational load versus classical two-body potentials. This is weighted against its out-of-the-box ability to obtain these results, with better results obtainable from a dedicated potential with more training data specific to the molten phase of LiF.

Our main interest was in the prediction of viscosity, using the same method as has been used in extant MD potentials (Buckingham and BHM) that is known to produce the correct trend but offset along the temperature axis for LiF. We have found that the MACE potential agrees well with experimental viscosities over a range of temperatures above melting. Further we have found that, when applying a naïve monotonic heating method-

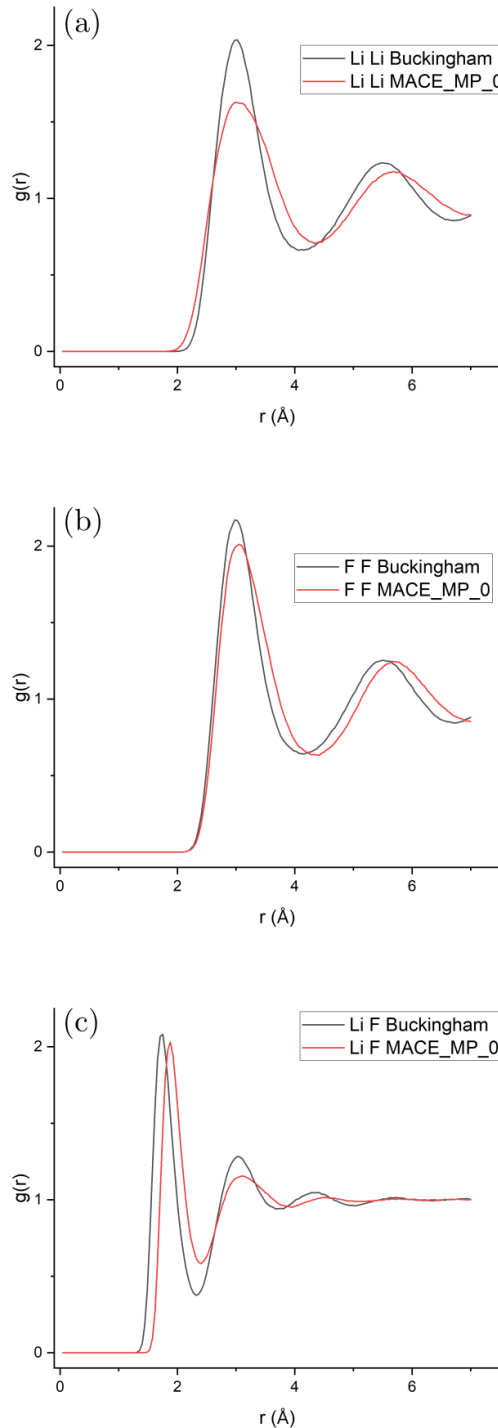


FIG. 4. Partial radial distribution functions (RDF) calculated for the respective melting temperatures of the potentials. 890K for Buckingham and 1147K for the MACE. (a) Lithium - Lithium , (b) Fluorine - Fluorine , (c) Lithium - Fluorine

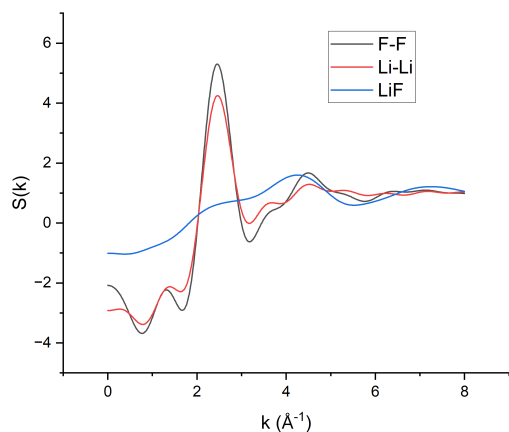


FIG. 5. $S(k)$ calculated at from the partial RDFs using 1000 MACE trajectory frames at 1147 K.

ology to crystalline LiF, the MACE potential is also able to recover the experimental melting temperature surprisingly accurately given the difficulty of ascertaining melting points in MD and DFT. The large discrepancy between the melting points of classical potentials and experiments has previously been the given explanation for the offset viscosity values. Our results lend some credence to that hypothesis, but it remains possible other effects such as system size and the lack of interfaces may contribute.

Looking to the system's structure and dynamics, our results indicate that the MACE potential generates a broader coordination environment around each ion, possibly reducing the stiffness of the aggregate interactions and thereby causing the decreased frequency in the oscillation of the Li atoms. The dynamics of the anions and cations are more similar in the MACE simulations, while in classical MD simulations they are quite distinct.

The far superior prediction of the viscosity and melting temperature of LiF indicate that the dynamics resulting the MACE potential, which differ qualitatively from those of classical potentials, are indispensable to the accurate simulation of this system. Dedicated potentials for the simulation of other molten salts and their mixtures will help guide experimentation and inform their application to industry.

ACKNOWLEDGEMENTS

We are grateful to EPSRC (for grant No. EP/W029006/1). This research utilised Queen Mary's Apocrita HPC facility, supported by QMUL Research-IT <http://doi.org/10.5281/zenodo.438045>, STFC Scientific Computing Department's SCARF cluster and the Sulis Tier 2 HPC platform hosted by the Scientific Computing Research Technology Platform at the University of War-

wick and funded by EPSRC Grants EP/T022108/1 and EP/V028537/1 and the HPC Midlands+ consortium.

- ¹N Papageorgiou, Y Athanassov, M Armand, P Bonho, H Pettersson, A Azam, Michael Grätzel, et al. The performance and stability of ambient temperature molten salts for solar cell applications. *Journal of the Electrochemical Society*, 143(10):3099, 1996.
- ²P. R. Kasten M. W. Rosenthal and R. B. Briggs. Molten-salt reactors—history, status, and potential. *Nuclear Applications and Technology*, 8(2):107–117, 1970. doi:10.13182/NT70-A28619. URL <https://doi.org/10.13182/NT70-A28619>.
- ³Benjamin A. Frandsen, Stella D. Nickerson, Austin D. Clark, Andrew Solano, Raju Baral, Johnny Williams, Jörg Neuefeind, and Matthew Memmott. The structure of molten flinak. *Journal of Nuclear Materials*, 537:152219, 2020. ISSN 0022-3115. doi:<https://doi.org/10.1016/j.jnucmat.2020.152219>. URL <https://www.sciencedirect.com/science/article/pii/S0022311520304736>.
- ⁴Todd Allen and D. Crawford. Lead-cooled fast reactor systems and the fuels and materials challenges. *Science and Technology of Nuclear Installations*, Dec 2007. doi:10.1155/2007/97486.
- ⁵Limei Tang, Ji Xiong, Weicai Wan, Zhixing Guo, Wei Zhou, Shiwei Huang, and Hua Zhong. The effect of fluid viscosity on the erosion wear behavior of ti(c,n)-based cermets. *Ceramics International*, 41(3, Part A):3420–3426, 2015. ISSN 0272-8842. doi:<https://doi.org/10.1016/j.ceramint.2014.10.141>. URL <https://www.sciencedirect.com/science/article/pii/S0272884214016939>.
- ⁶U.S. Nuclear Regulatory Commission. General electric systems technology manual: Water cooled reactors. <https://www.nrc.gov/docs/ML1125/ML11258A291.pdf>, 2011.
- ⁷Elsa Merle, Daniel Heuer, M. Allibert, X. Doligez, and Veronique Ghetta. Minimizing the fissile inventory of the molten salt fast reactor. *American Nuclear Society - 4th Topical Meeting on Advances in Nuclear Fuel Management 2009, ANFM IV*, 1, 04 2009.
- ⁸Giorgio Locatelli, Mauro Mancini, and Nicola Todeschini. Generation iv nuclear reactors: Current status and future prospects. *Energy Policy*, 61:1503–1520, 10 2013. ISSN 0301-4215. doi:10.1016/J.ENPOL.2013.06.101.
- ⁹Mathieu Salanne, Christian Simon, Pierre Turq, and Paul A. Madden. Calculation of activities of ions in molten salts with potential application to the pyroprocessing of nuclear waste. *Journal of Physical Chemistry B*, 112:1177–1183, 1 2008. ISSN 15206106. doi:10.1021/JP075299N/ASSET/IMAGES/MEDIUM/JP075299NE00018.GIF. URL <https://pubs.acs.org/doi/full/10.1021/jp075299n>.
- ¹⁰Koichi Uozumi, Masatoshi Iizuka, and Takashi Omori. Removal of rare-earth fission products from molten chloride salt used in pyroprocessing by precipitation for consolidation into glass-bonded sodalite waste form. *Journal of Nuclear Materials*, 547:152784, 4 2021. ISSN 0022-3115. doi:10.1016/J.JNUCMAT.2021.152784.
- ¹¹Hansoo Lee, Geun Il Park, Kweon Ho Kang, Jin Mok Hur, Jeong Guk Kim, Do Hee Ahn, Yung Zun Cho, and Eung Ho Kim. Pyroprocessing technology development at kaeri. *Nuclear Engineering and Technology*, 43:317–328, 2011. ISSN 1738-5733. doi:10.5516/NET.2011.43.4.317. URL <http://dx.doi.org/10.5516/NET.2011.43.4.317>.
- ¹²Koshi Mitachi and Yoichiro Shimazu. Incineration of transuranium elements using chlorides molten salt fast reactors – a proposal of incineration in three steps. *Journal of Nuclear Science and Technology*, 59:1297–1303, 10 2022. ISSN 00223131. doi:10.1080/00223131.2022.2045232. URL <https://www.tandfonline.com/doi/abs/10.1080/00223131.2022.2045232>.
- ¹³Adrián Caraballo, Santos Galán-Casado, Ángel Caballero, and Sara Serena. Molten salts for sensible thermal energy storage: A review and an energy performance analysis. *Energies 2021, Vol. 14, Page 1197*, 14:1197, 2 2021. ISSN 1996-1073. doi:

- 10.3390/EN14041197. URL <https://www.mdpi.com/1996-1073/14/4/1197/htm><https://www.mdpi.com/1996-1073/14/4/1197>.
- ¹⁴Pranshul Bhatnagar, Sufiyan Siddiqui, Inkollu Sreedhar, and Rajagopalan Parameshwaran. Molten salts: Potential candidates for thermal energy storage applications. *International Journal of Energy Research*, 46:17755–17785, 10 2022. ISSN 1099-114X. doi:10.1002/ER.8441. URL <https://onlinelibrary.wiley.com/doi/full/10.1002/er.8441><https://onlinelibrary.wiley.com/doi/abs/10.1002/er.8441><https://onlinelibrary.wiley.com/doi/10.1002/er.8441>.
- ¹⁵Zhen Yang and Suresh V. Garimella. Thermal analysis of solar thermal energy storage in a molten-salt thermocline. *Solar Energy*, 84:974–985, 6 2010. ISSN 0038-092X. doi:10.1016/j.solener.2010.03.007.
- ¹⁶Thomas Bauer, Christian Odenthal, and Alexander Bonk. Molten salt storage for power generation. *Chemie Ingenieur Technik*, 93(4):534–546, 2021.
- ¹⁷K. Trachenko. Properties of condensed matter from fundamental physical constants. *Advances in Physics*, 70:469, 2023.
- ¹⁸K. Trachenko. *Theory of Liquids: from Excitations to Thermodynamics*. Cambridge University Press, 2023.
- ¹⁹A. V. Granato. The specific heat of simple liquids. *Journal of Non-Crystalline Solids*, 307-310:376, 2002.
- ²⁰J. Proctor. Modeling of liquid internal energy and heat capacity over a wide pressure–temperature range from first principles. *Phys. Fluids*, 32:107105, 2020.
- ²¹G. Chen. Perspectives on molecular-level understanding of thermophysics of liquids and future research directions. *Journal of Heat Transfer*, 144:010801, 2022.
- ²²K. Trachenko and V. V. Brazhkin. Minimal quantum viscosity from fundamental physical constants. *Sci. Adv.*, 6:aba3747, 2020.
- ²³M. Withington, H. L. Devereux, C. Cockrell, A. M. Elena, I. T. Todorov, Z. K. Liu, S. L. Shang, J. S. McCloy, P. A. Bingham, and K. Trachenko. Viscosity bounds in liquids with different structure and bonding types. *Phys. Rev. B*, 109:094205, Mar 2024. doi:10.1103/PhysRevB.109.094205. URL <https://link.aps.org/doi/10.1103/PhysRevB.109.094205>.
- ²⁴Hui Luo, Shifang Xiao, Shengjie Wang, Ping Huai, Huiqiu Deng, and Wangyu Hu. Molecular dynamics simulation of diffusion and viscosity of liquid lithium fluoride. *Computational Materials Science*, 111:203–208, 2016. ISSN 0927-0256. doi:<https://doi.org/10.1016/j.commatsci.2015.09.052>. URL <https://www.sciencedirect.com/science/article/pii/S0927025615006333>.
- ²⁵R. A. Buckingham and John Edward Lennard-Jones. The classical equation of state of gaseous helium, neon and argon. *Proceedings of the Royal Society of London. Series A. Mathematical and Physical Sciences*, 168 (933):264–283, 1938. doi:10.1098/rspa.1938.0173. URL <https://royalsocietypublishing.org/doi/abs/10.1098/rspa.1938.0173>.
- ²⁶M.P. Tosi and F.G. Fumi. Ionic sizes and born repulsive parameters in the nacl-type alkali halides—ii: The generalized huggins-mayer form. *Journal of Physics and Chemistry of Solids*, 25(1): 45–52, 1964. ISSN 0022-3697. doi:[https://doi.org/10.1016/0022-3697\(64\)90160-X](https://doi.org/10.1016/0022-3697(64)90160-X). URL <https://www.sciencedirect.com/science/article/pii/002236976490160X>.
- ²⁷M.J.L. Sangster and M. Dixon. Interionic potentials in alkali halides and their use in simulations of the molten salts. *Advances in Physics*, 25(3):247–342, 1976. doi:10.1080/00018737600101392. URL <https://doi.org/10.1080/00018737600101392>.
- ²⁸G. Ciccotti, G. Jacucci, and I. R. McDonald. Transport properties of molten alkali halides. *Phys. Rev. A*, 13:426–436, Jan 1976. doi:10.1103/PhysRevA.13.426. URL <https://link.aps.org/doi/10.1103/PhysRevA.13.426>.
- ²⁹Ilyes Batatia, David Peter Kovacs, Gregor N. C. Simm, Christoph Ortner, and Gabor Csanyi. MACE: Higher order equivariant message passing neural networks for fast and accurate force fields. In Alice H. Oh, Alekh Agarwal, Danielle Belgrave, and Kyunghyun Cho, editors, *Advances in Neural Information Processing Systems*, 2022. URL <https://openreview.net/forum?id=YPPsNgE-ZU>.
- ³⁰Ilyes Batatia, Simon Batzner, Dávid Péter Kovács, Albert Musaelian, Gregor N. C. Simm, Ralf Drautz, Christoph Ortner, Boris Kozinsky, and Gábor Csányi. The design space of e(3)-equivariant atom-centered interatomic potentials, 2022.
- ³¹Ilyes Batatia, Philipp Benner, Yuan Chiang, Alin M Elena, Dávid P Kovács, Janosh Riebesell, Xavier R Advincula, Mark Asta, William J Baldwin, Noam Bernstein, et al. A foundation model for atomistic materials chemistry. *arXiv preprint arXiv:2401.00096*, 2023.
- ³²I. T. Todorov, W. Smith, K. Trachenko, and M.T. Dove. DL-poly.3: new dimensions in molecular dynamics simulations via massive parallelism. *J. Mater. Chem.*, 16:1911, 2006.
- ³³Kasoar Elliott, Zanca Federica, Wilkins Jacob, Devereux Harvey, Mason David, Austen Patrick, and Elena Alin. janus-core, October 2024. URL <https://doi.org/10.5281/zenodo.14001356>.
- ³⁴Robert Zwanzig and Raymond D. Mountain. High-frequency elastic moduli of simple fluids. *The Journal of Chemical Physics*, 43:4464–4471, 12 1965. ISSN 00219606. doi:10.1063/1.1696718. URL <http://aip.scitation.org/doi/10.1063/1.1696718>.
- ³⁵Mark E Tuckerman. *Statistical mechanics: theory and molecular simulation*. Oxford university press, 2023.
- ³⁶Yong Zhang, Akihito Otani, and Edward J Maginn. Reliable viscosity calculation from equilibrium molecular dynamics simulations: A time decomposition method. *Journal of chemical theory and computation*, 11(8):3537–3546, 2015.
- ³⁷Ask Hjorth Larsen, Jens Jørgen Mortensen, Jakob Blomqvist, Ivano E Castelli, Rune Christensen, Marcin Dułak, Jesper Friis, Michael N Groves, Bjørk Hammer, Cory Hargus, Eric D Hermes, Paul C Jennings, Peter Bjerre Jensen, James Kermode, John R Kitchin, Esben Leonhard Kolsbjerg, Joseph Kubal, Kristen Kaasbjerg, Steen Lysgaard, Jón Bergmann Maronsson, Tristan Maxson, Thomas Olsen, Lars Pastewka, Andrew Peterson, Carsten Rostgaard, Jakob Schiøtz, Ole Schütt, Mikkel Strange, Kristian S Thygesen, Tejs Vegge, Lasse Vilhelmsen, Michael Walter, Zhenhua Zeng, and Karsten W Jacobsen. The atomic simulation environment—a python library for working with atoms. *Journal of Physics: Condensed Matter*, 29(27):273002, 2017. URL <http://stacks.iop.org/0953-8984/29/i=27/a=273002>.
- ³⁸U. (Umberto) Balucani and Marco Zoppi. *Dynamics of the liquid state*. Clarendon Press, 1994. ISBN 9780198517399. URL <https://global.oup.com/academic/product/dynamics-of-the-liquid-state-9780198517399?cc=gb&lang=en&>.
- ³⁹C. Cockrell, V. V. Brazhkin, and K. Trachenko. Universal interrelation between dynamics and thermodynamics and a dynamically driven “c” transition in fluids. *Phys. Rev. E*, 104: 034108, Sep 2021. doi:10.1103/PhysRevE.104.034108. URL <https://link.aps.org/doi/10.1103/PhysRevE.104.034108>.
- ⁴⁰George J Janz. *Physical properties data compilations relevant to energy storage*. US Department of Commerce, National Bureau of Standards, 1977.
- ⁴¹Yoshiyuki Abe, Otoyá Kosugiyama, and Akira Nagashima. Viscosity of lif-bef₂ eutectic mixture (xbef₂ = 0.328) and lif single salt at elevated temperatures. *Journal of Nuclear Materials*, 99(2):173–183, 1981. ISSN 0022-3115. doi:[https://doi.org/10.1016/0022-3115\(81\)90186-0](https://doi.org/10.1016/0022-3115(81)90186-0). URL <https://www.sciencedirect.com/science/article/pii/0022311581901860>.
- ⁴²Tatsuhiko Ejima, Yuzuru Sato, Seiji Yaegashi, Takashi Kijima, Eiji Takeuchi, and Kyōko Tamai. Viscosity of molten alkali fluorides. *Journal of The Japan Institute of Metals*, 51:328–337, 1987. URL <https://api.semanticscholar.org/CorpusID:99027309>.
- ⁴³Ana-Maria Popescu and Virgil Constantin. Viscosity of alkali fluoride ionic melts at temperatures up to 373.15 k above melting points. *Chemical Engineering Communications*, 202(12):1703–1710, 2015. doi:10.1080/00986445.2014.970254. URL <https://>

- doi.org/10.1080/00986445.2014.970254.
- ⁴⁴Ulrich Essmann, Lalith Perera, Max L Berkowitz, Tom Darden, Hsing Lee, and Lee G Pedersen. A smooth particle mesh ewald method. *The Journal of chemical physics*, 103(19):8577–8593, 1995.
- ⁴⁵Noam Bernstein. From gap to ace to mace. *arXiv preprint arXiv:2410.06354*, 2024.
- ⁴⁶Bowen Deng, Peichen Zhong, KyuJung Jun, Janosh Riebesell, Kevin Han, Christopher J Bartel, and Gerbrand Ceder. Chgnet as a pretrained universal neural network potential for charge-informed atomistic modelling. *Nature Machine Intelligence*, 5(9):1031–1041, 2023.
- ⁴⁷Anubhav Jain, Shyue Ping Ong, Geoffroy Hautier, Wei Chen, William Davidson Richards, Stephen Dacek, Shreyas Cholia, Dan Gunter, David Skinner, Gerbrand Ceder, et al. Commentary: The materials project: A materials genome approach to accelerating materials innovation. *APL materials*, 1(1), 2013.
- ⁴⁸Material project, matbench discovery. <https://matbench-discovery.materialsproject.org/>. Accessed: 2024-10-24.
- ⁴⁹Thomas B Douglas and James L Dever. Lithium fluoride: Heat content from 0 to 900°, the melting point and heat of fusion. *Journal of the American Chemical Society*, 76(19):4826–4829, 1954.
- ⁵⁰David R Lide. *CRC handbook of chemistry and physics*, volume 85. CRC press, 2004.
- ⁵¹MG Mead. Comparison of the optical and dielectric properties of crystalline and molten lithium fluoride. *Journal of Physics C: Solid State Physics*, 7(2):445, 1974.
- ⁵²Dario Corradini, Dario Marrocchelli, Paul A Madden, and Mathieu Salanne. The effect of dispersion interactions on the properties of lif in condensed phases. *Journal of Physics: Condensed Matter*, 26(24):244103, 2014.
- ⁵³Oliver J Lanning, Stephen Shellswell, and Paul A Madden*. Solid–liquid coexistence in ionic systems and the properties of the interface. *Molecular Physics*, 102(9-10):839–855, 2004.
- ⁵⁴D Frenkel and B. Smit. *Understanding molecular simulation: from algorithms to applications*, volume 2. Academic Press San Diego, 2002.
- ⁵⁵D Alfè, MJ Gillan, and GD Price. Complementary approaches to the ab initio calculation of melting properties. *The Journal of chemical physics*, 116(14):6170–6177, 2002.
- ⁵⁶Mauro C. C. Ribeiro. Chemla effect in molten licl/kcl and lif/kf mixtures. *The Journal of Physical Chemistry B*, 107(18):4392–4402, 2003. doi:10.1021/jp027261a. URL <https://doi.org/10.1021/jp027261a>.
- ⁵⁷C. Cockrell, V. V. Brazhkin, and K. Trachenko. Transition in the supercritical state of matter: review of experimental evidence. *Physics Reports*, 941:1, 2021.
- ⁵⁸Maria C Abramo, Dino Costa, Gianpietro Malescio, Gianmarco Munaò, Giuseppe Pellicane, Santi Prestipino, and Carlo Caccamo. Structure factors and x-ray diffraction intensities in molten alkali halides. *Journal of Physics Communications*, 4(7):075017, 2020.